

## **General Disclaimer**

### **One or more of the Following Statements may affect this Document**

- This document has been reproduced from the best copy furnished by the organizational source. It is being released in the interest of making available as much information as possible.
- This document may contain data, which exceeds the sheet parameters. It was furnished in this condition by the organizational source and is the best copy available.
- This document may contain tone-on-tone or color graphs, charts and/or pictures, which have been reproduced in black and white.
- This document is paginated as submitted by the original source.
- Portions of this document are not fully legible due to the historical nature of some of the material. However, it is the best reproduction available from the original submission.



## Technical Memorandum 79601

# Monitoring Changes in Upper Ocean Heat Storage from Satellites

(NASA-TM-79601) MONITORING CHANGES IN UPPER  
OCEAN HEAT STORAGE FROM SATELLITES (NASA)  
35 p HC A03/MF A01 CSCI 08J

W78-30793

G3/48 Unclass  
29346

James R. Miller

JULY 1978

National Aeronautics and  
Space Administration

**Goddard Space Flight Center**  
Greenbelt, Maryland 20771



**TM 79601**

**MONITORING CHANGES IN UPPER OCEAN  
HEAT STORAGE FROM SATELLITES**

**James R. Miller**

**Department of Meteorology and Physical Oceanography**

**Cook College, Rutgers University**

**New Brunswick, New Jersey 08903**

**July 1978**

**GODDARD SPACE FLIGHT CENTER**

**Greenbelt, Maryland 20771**

# **MONITORING CHANGES IN UPPER OCEAN HEAT STORAGE FROM SATELLITES**

**James R. Miller**

**Department of Meteorology and Physical Oceanography  
Cook College, Rutgers University  
New Brunswick, New Jersey 08903**

## **ABSTRACT**

The development of new oceanographic satellites such as SEASAT-A will provide measurements applicable to studies of heat storage changes in the upper ocean on seasonal and annual time scales. A one-dimensional model of the upper ocean mixed-layer has been developed to determine how the parameters which can be measured from satellites affect the development of the layer. The results show that the form of the dissipation term is important in achieving cyclic annual states, that the layer deepening rate depends on the averaging period for the surface heat flux and wind stress, that wind direction, as well as magnitude, can affect the deepening rate and that horizontal advective effects cannot simply be superimposed on the model results. An algorithm is given which uses satellite derived wind stress and sea surface temperature data to predict real time changes in upper ocean heat storage during the cooling seasons.

## CONTENTS

	<u>Page</u>
1. INTRODUCTION . . . . .	1
2. MODEL DESCRIPTION . . . . .	2
3. DIURNAL AND ANNUAL CYCLES . . . . .	7
4. SURFACE WIND STRESS . . . . .	10
5. ADVECTIVE EFFECTS . . . . .	12
6. SUMMARY AND CONCLUSIONS . . . . .	13
1. Annual Cycle . . . . .	14
2. Diurnal Cycle and Data Averaging . . . . .	14
3. Vector Wind Stress . . . . .	14
4. Forced and Free Convection . . . . .	14
5. Horizontal Advection . . . . .	15
ACKNOWLEDGMENTS . . . . .	15
REFERENCES . . . . .	27

## ILLUSTRATIONS

<u>Figure</u>		<u>Page</u>
1	Flight Configuration of SEASAT-A with Location of Various Sensors. .	16
2	Schematic Representation of the Temperature Profile Assumed in the Mixed-Layer Model. Relevant Parameters Are the Sea Surface Temperature (T), the Mixed-Layer Depth (h), the Temperature Immediately Below the Mixed-Layer ( $T_h$ ), and the Temperature Gradient $\left(\frac{\partial T}{\partial z}\right)$ in the Lower Region . . . . .	17
3	Comparison of Mixed-Layer Deepening With and Without Background Dissipation. There is No Net Heating and the Wind Speed is Constant at 10 m sec <sup>-1</sup> . . . . .	18
4	Variations in Annual Cyclic States Due to Changes in the Background Dissipation and Penetrative Convection Terms. The Heat Flux is Sinusoidal with a One-Year Period and an Amplitude of 400 cal cm <sup>-2</sup> day <sup>-1</sup> . The Wind Speed is 10 m sec <sup>-1</sup> . . . . .	19
5	Variations in Deepening Rates Due to Changes in the Averaging Interval for the Surface Heat Fluxes. The Net Heating is Zero and the Wind Speed is 8 m sec <sup>-1</sup> . For Curve A, the Heat Flux is Zero throughout the Period While the Heat Flux Varies Sinusoidally with an Amplitude of 960 cal cm <sup>-2</sup> day <sup>-1</sup> and an Averaging Interval of 1.2 Hours for the Other Two Curves . . . . .	20

## ILLUSTRATIONS (Continued)

<u>Figure</u>		<u>Page</u>
6	Variations of Sea Surface Temperature Due to Using Different Averaging Periods for the Surface Heat Fluxes ( $m_b = 0$ , $m_c = 1$ ) . . . .	21
7	Variations in Mixed-Layer Deepening Over Ten Diurnal Cycles With and Without Background Dissipation. Curve B is the Same as Curve B in Figure 5 . . . . .	22
8	Solid Curve Shows Mixed-Layer Deepening Due to an Impulsive Wind Stress with $u = 5 \text{ m sec}^{-1}$ Except During the Impulsive Event. The Other Two Curves Show the Different Deepening Rates When Different Averaging Methods Are Used . . . . .	23
9	Effect of Wind Direction on the Mixed-Layer Deepening Rate When a $10 \text{ cm sec}^{-1}$ Current in the Positive x-Direction is Initially Present . .	24
10	Schematic Diagram of an Algorithm for Predicting Real Time Changes of the Heat Storage of the Upper Ocean Using SEASAT Wind Speed and Sea Surface Temperature Data. An Additional Output is a Measure of the Heat Flux Between Successive Satellite Passes. This Case is for a Cooling Regime with $\frac{\partial T}{\partial z} = 0$ Below the Mixed-Layer and Assuming a Time Interval of One Unit . . . . .	25
11	Variation in Mixed-Layer Depth Due to the Advection of Warmer Water Through the Region . . . . .	26

# **MONITORING CHANGES IN UPPER OCEAN HEAT STORAGE FROM SATELLITES**

## **1. INTRODUCTION**

The development of the SEASAT-A and Nimbus G satellites will provide a wealth of new information about the physical processes occurring at the air-sea interface. SEASAT will have a complement of microwave sensors to measure such parameters as sea surface temperature, surface currents, sea ice and scalar and vector wind stress at the sea surface. Figure 1 shows the flight configuration and the various sensors that will be aboard the spacecraft. The purpose here is to consider how measurement of these parameters can be utilized by oceanographers and climatologists who are interested in the development of the upper ocean mixed-layer and the corresponding change in heat storage on seasonal and annual time scales. In order to understand how climatic variations occur on these time scales, it is essential to know how heat is stored in the upper ocean. For these studies the two principal instruments on SEASAT are the SEASAT-A Scatterometer System (SASS), an active sensor that measures sea surface wind stress, and the Scanning Multifrequency Microwave Radiometer (SMMR), a passive sensor which will provide sea surface temperatures.

A model which faithfully reproduces the seasonal and annual evolution of the ocean surface mixed-layer is particularly important to climate modelers who must know whether heat fluxes across the air-sea interface are distributed through a shallow surface layer or through a much deeper layer. The heat storage varies both temporally and spatially, and it is affected by such physical processes as the surface wind stress, heat fluxes at the air-sea interface, horizontal advection and deep ocean processes. Since the deep ocean processes cannot be observed directly from satellites, such processes will not be considered here. Ultimately it may be possible to use satellite data to accurately predict the heat storage in the upper ocean, and this information may in turn be used in climate models to provide realistic climate predictions.



One of the first models of the ocean mixed-layer was developed by Munk and Anderson (1948). Kraus and Turner (1967) developed a one-dimensional model of the seasonal thermocline, that was generalized by Denman (1973) to consider a time-dependent problem. These models are concerned primarily with determining how mechanical mixing causes the mixed-layer to move downward by entraining denser water from below. Pollard, Rhines and Thompson (1973) invoked a Richardson number criterion at the entraining interface. Miller (1976) showed that in certain situations the salinity structure, rather than the thermal structure, could control the rate of deepening. Since satellites are capable of measuring the physical parameters responsible for mixed-layer deepening, namely wind stress and heat fluxes, it is quite appropriate to consider these one-dimensional models and their ability to simulate changes in the heat storage of the upper ocean. Thompson (1976) has shown that these one-dimensional models can predict the annual development of the mixed-layer at a mid-latitude location.

In the next section a one-dimensional model of the ocean mixed-layer is developed. In subsequent sections various aspects of the model are discussed in the context of utilizing satellite measurements to improve the real time predictability of changes in the heat storage of the upper ocean. Problems associated with the discontinuous coverage by satellites and the subsequent need to insert spatially and temporally averaged data are discussed. An algorithm is presented which shows how SEASAT wind stress and sea surface temperature data can be used to predict changes in mixed-layer depth between successive passes of the satellite. An additional output parameter is a measure of the heat fluxes between two satellite passes. Finally, the effects of horizontal advection on the dynamics of the mixed-layer are briefly considered.

## 2. MODEL DESCRIPTION

A good review of one-dimensional models of the upper ocean can be found in a paper by Miller and Kraus (1977). These time-dependent models assume the existence of a mixed-layer

of depth  $h$ , through which the density and horizontal velocity are uniform. Discontinuities in density and horizontal velocity are assumed across the bottom of the mixed-layer, and a linear density gradient occurs in the region below. Only the effects of temperature on the density structure will be considered here, although Miller (1976) has shown that the salinity effect can be quite important in subtropical regions. Figure 2 shows the structure of the mixed-layer that will be assumed throughout this paper.

The fundamental parameters that describe the characteristics of the mixed-layer are the temperature and depth. A system of ordinary differential equations for these parameters depends on the time-dependent boundary conditions which consist of the surface wind stress, sensible and latent heat fluxes, incident solar radiation and the net longwave back radiation. These ordinary differential equations are derived by integrating the equations for conservation of heat and turbulent mechanical energy across the mixed-layer.

The equation for the conservation of heat is based on the first law of thermodynamics, and its time averaged turbulent form is given by

$$\frac{\partial T}{\partial t} + u \frac{\partial T}{\partial x} + v \frac{\partial T}{\partial y} + w \frac{\partial T}{\partial z} + \frac{\partial}{\partial z} (\overline{w'T'}) = \frac{1}{\rho c} \frac{\partial Q}{\partial z}, \quad (1)$$

where  $T$  is the mean temperature of the mixed-layer,  $w'$  and  $T'$  are fluctuating components of the vertical velocity and the temperature,  $\rho$  is the water density,  $c$  is the specific heat,  $Q(z)$  is a depth dependent heat source term due to solar radiation, and  $u$ ,  $v$  and  $w$  are mean velocities in the  $x$ ,  $y$ , and  $z$  directions, respectively. In the following, the vertical velocity  $w$  will be assumed to be zero, although it can easily be incorporated to account for upwelling across the bottom of the mixed-layer. The horizontal velocities will also be assumed zero except in Section 5 where the effects of advection will be discussed. The boundary conditions for heat flux across the upper and lower boundaries are given by

$$(\overline{w'T'})_{z=0} = \frac{-F_{\star}}{\rho c} = -F \quad (2)$$

and

$$(\overline{w'T'})_{z=-h} = -\frac{dh}{dt} (T - T_h) \quad (3)$$

where  $F_\star$  is the sum of the sensible and latent heat fluxes and the net longwave back radiation and  $T_h$  is the temperature immediately below the mixed-layer.

The turbulent kinetic energy equation for a horizontally homogeneous ocean is given by Phillips (1966) as

$$\begin{aligned} \frac{\partial}{\partial t} \left( \frac{1}{2} \overline{c^2} \right) = & -\overline{u'w'} \frac{\partial u}{\partial z} - \overline{v'w'} \frac{\partial v}{\partial z} - \frac{\partial}{\partial z} \left[ \overline{w' \left( \frac{p'}{\rho} + \frac{c^2}{2} \right)} \right] \\ & - \alpha g (\overline{w'T'}) - \epsilon, \end{aligned} \quad (4)$$

where  $\frac{1}{2} \overline{c^2} \equiv \frac{1}{2} (\overline{u'^2 + v'^2 + w'^2})$  is the mean kinetic energy of the turbulent motion,

$p'$  is the pressure perturbation,  $g$  is the gravitational acceleration,  $\alpha$  is the coefficient of thermal expansion and  $\epsilon$  is the dissipation term. The first two terms on the r.h.s. of Eq. (4) represent the production of turbulent energy by the Reynolds stresses acting on the mean velocity shear. The third term represents the divergence of the vertical transports of turbulent energy, and the fourth term,  $\alpha g (\overline{w'T'})$  represents a loss of energy in a stably stratified fluid due to work done against the density gradient. The density has been eliminated from the buoyancy term by assuming that  $\rho = \rho_0 (1 + \alpha (T - T_0))$ , where  $\rho_0$  and  $T_0$  are reference densities and temperatures respectively.

The principal differences among the various one-dimensional models arise due to different parameterizations of the turbulent kinetic energy equation (Eq. 4), particularly the parameterization of the dissipation term. Niiler (1975) used a three layer model to resolve deepening events due to velocity shear and derived the following expression for the integrated turbulent production:

$$\begin{aligned}
& - \int_{-h}^0 \left( (\overline{u'w'}) \frac{\partial u}{\partial z} + (\overline{v'w'}) \frac{\partial v}{\partial z} \right) dz - \overline{w' \left( \frac{p'}{\rho} + \frac{c^2}{2} \right)}_{z=0} \\
& = m u_{\star}^3 + \frac{\bar{u}^2}{2} \frac{dh}{dt}, \tag{5}
\end{aligned}$$

where  $m$  is a constant,  $\bar{u}$  is the average velocity through the mixed-layer and  $u_{\star}$  is the friction velocity. If Eq. (1) is integrated from 0 to  $z$  and then integrated again across the mixed-layer, the expression for the integrated vertical buoyancy flux is

$$\int_{-h}^0 \overline{w'T'} dz = - \frac{h}{2} (F + R) + \gamma^{-1} R - \frac{1}{2} h \Delta T \frac{dh}{dt} \tag{6}$$

$R$  is the solar radiation transmitted across the air-sea interface,  $\Delta T$  is the temperature jump across the bottom of the mixed-layer, and  $\gamma$  is the solar extinction coefficient. The integrated dissipation is assumed to have the form

$$\begin{aligned}
\int_{-h}^0 \epsilon dz &= m_p u_{\star}^3 + \frac{m_s}{2} \frac{dh}{dt} \bar{u}^2 + a g (1 - m_c) \frac{1}{2} h (F + R) \\
&+ m_b h \tag{7}
\end{aligned}$$

where the constants  $m_p$ ,  $m_s$ ,  $m_c$  and  $m_b$  are related to dissipation balancing the production, shear at the bottom interface, convection and a background dissipation, respectively. The above expression appears in the paper of Niiler and Kraus with the constant  $m_b = 0$ . Kim (1976) included the last term in Eq. (7) and assumed a value of  $m_b = 2 \times 10^{-6} \text{ m}^2 \text{ sec}^{-3}$ . The third term on the r.h.s. of Eq. (7) was suggested by Gill and Turner (1976) to limit penetrative deepening during the cooling season. The constant  $m_s$  was set to zero by Niiler, but Wyatt (1976) has suggested a non-zero value for  $m_s$  to allow for shear dissipation at the bottom boundary.

An equation for the time rate of change of the mixed-layer depth can now be obtained by integrating Eq. (4) from  $z = 0$  to  $z = h$  and substituting Eqs. (5), (6) and (7) to yield

$$\begin{aligned} \frac{dh}{dt} \left[ -\frac{\alpha g h}{2} (T - T_h) - (1 - m_s) \frac{\bar{u}^2}{2} \right] = (m - m_p) u_*^3 \\ - \alpha g \gamma^{-1} R + m_c \frac{\alpha g h}{2} (F + R) - m_b h. \end{aligned} \quad (8)$$

The l.h.s. of Eq. (4) is assumed to be small for the time scales of interest. Substitution of Eqs. (2) and (3) into the integrated form of Eq. (1) leads to an equation for the rate of change of the surface temperature given by

$$\frac{dT}{dt} = \frac{1}{h} \left[ -\frac{dh}{dt} (T - T_h) + F + R \right]. \quad (9)$$

Assuming that the structure below the mixed-layer remains constant in time, the equation for  $T_h$  is

$$\frac{dT_h}{dt} = -L \frac{dh}{dt}, \quad (10)$$

where  $L$  is the temperature gradient below the mixed-layer.

Whenever there is not sufficient production of turbulent kinetic energy to produce mixed-layer deepening, then the r.h.s. of (8) is set equal to zero and solved for  $h$ . It should be noted that during a heating regime ( $F + R > 0$ ),  $m_c = 1$ . In the next sections, sensitivity studies, as well as the effects of various terms in Eq. (8), will be analyzed with particular emphasis on determining how satellite data can be used to aid in real time prediction of the variations of heat content in the upper ocean.

### 3. DIURNAL AND ANNUAL CYCLES

One of the principal weaknesses of the one-dimensional Kraus and Turner model is that too much deepening occurs during the cooling season. That model is given by Eq. (8) with  $m_s = m_c = 1$  and  $m_b = 0$ . To properly simulate the annual cycle, it is necessary to model the dissipation term given by Eq. (7) in a more realistic way. One method, proposed by Kim (1976), involves setting  $m_b = 2 \times 10^{-8} \text{ m}^2 \text{ sec}^{-3}$  to allow for a constant background dissipation. Figure 3 shows how the inclusion of this term significantly reduces the deepening over a 60 day period when the wind stress and the surface cooling remain the same for both cases. Without the background dissipation term the layer deepens by more than 100 m, whereas inclusion of the term limits the total deepening to about 50 m.

Over an annual cycle for which the heat fluxes and wind stress are set equal to the climatological values, it is desirable that the mixed-layer depth and the heat storage return to their initial values at the end of the cycle. Figure 4 shows three different model simulations assuming a sinusoidal heat flux with a one year period and a constant wind stress. Curve A shows the excessive deepening that occurs during the cooling season when the Kraus and Turner model is used. Gill and Turner (1976) have suggested that the deepening during the cooling season can be reduced by considering a model that does not include fully penetrative convection. Curve B shows that the deepening is considerably reduced when no penetrative convection is allowed (i.e.  $m_c = 0$ ). A more realistic model would allow for a positive, but small, value of  $m_c$ . Finally, curve C shows the effect of including a background dissipation with no penetrative convection allowed. In this case the mixed-layer returns to the same depth as the initial depth and a cyclic annual state is achieved.

Any models that purport to use satellite data to model either seasonal or annual changes of the heat storage in the upper ocean must include a parameterization of the dissipation term. Although the choice of a non-zero value of  $m_b$  can produce annual cyclic states, Niiler and Kraus (1977) find little physical justification for its inclusion and set it to zero. Since this

still leads to too much deepening during the cooling season, even with  $m_c = 0$  in curve B of Fig. 4, it appears reasonable to assume that  $m - m_p$  in Eq. (8) becomes smaller as the layer deepens during the cooling season. More research is required with respect to analysis of observational data to determine the relative importance of forced and free convection during the cooling season.

In addition to the variation in heat flux over an annual cycle, a much shorter time scale variation occurs due to the diurnal variation of the incident solar radiation. Since satellites do not provide continuous coverage of the incident solar radiation at specific ocean sites, the radiation data must be inserted into the model in an averaged form. Figure 5 shows the mixed-layer depth variation for a ten day period using different averaging techniques for the radiation. In all three cases there is no net heating during the three day period. Curve A shows the gradual deepening which occurs for a constant wind stress when the average heat flux is constant and equal to zero. For curves B and C, the incident solar radiation,  $R$ , varies sinusoidally over the daily cycle with the proviso that when  $R$  is negative  $F$  is set equal to  $R$  and  $R$  set to zero in Eq. (8). Hence, over a daily cycle, the net heat flux is zero. More deepening occurs for curve B because penetrative convection occurs along with the wind deepening during the cooling period (i.e.  $m_c = 1$ ). If the penetrative convection at night is eliminated by setting  $m_c = 0$ , then the net deepening is significantly reduced as shown by curve C. In both B and C, a diurnal variation of the mixed-layer depth occurs as the solution of Eq. (8) alternately shifts between heating and cooling regimes. The important point in regard to satellite inputs to the model is that different depths are predicted at the end of a ten day period depending on the choice of averaging period as well as on the penetrative convection constant,  $m_c$ . These changes in depth will be accompanied by different surface temperature variations for the different averaging periods.

Figure 6 shows that the variations of surface temperature differ over the ten day period depending on the time period over which the heat fluxes are averaged. Curves A and B

correspond to the mixed-layer depth variations of curves A and B in Fig. 5. In all cases the net heating due to surface heat fluxes over the ten day period is zero. Curves B and C show that in addition to the diurnal variation of sea surface temperature, a gradual decrease in the average temperature also occurs. Figure 6 indicates that a greater overall temperature decrease occurs when the shorter averaging periods are used. This greater decrease can be explained by comparison with Fig. 5 which shows that the shorter averaging period leads to deeper depths and hence greater entrainment of colder water from below.

Figure 7 shows that two additional features arise if the background dissipation is included in the diurnal simulation. With  $m_b > 0$ , a shallower mixed-layer forms during the heating regime, and less deepening occurs at the end of the ten day period. Curve B is the same in Figs. 5 and 7. The shallower depth occurs due to the additional term which arises when the r.h.s. of Eq. (8) is set to zero during the heating regime.

The extinction coefficient  $\gamma$  also affects the characteristics of the heating regime. Increasing the value of  $\gamma$  will cause shallower mixed-layers to form during the heating regime and thus lead to greater temperature variations in the surface mixed-layer. Alexander and Kim (1976) analyzed the summer heating regime for the North Pacific Ocean and found it necessary to use a somewhat larger extinction coefficient than suggested by Jerlov (1968) in their one-dimensional model.

Since the heat flux terms at the air-sea interface vary both spatially and temporally, it will be extremely difficult to provide real time monitoring of these fluxes with satellites. It will be necessary to supplement the real time observations with assumptions based on persistence, climatology, spatial correlations or some combination of these to provide a continuous record of the heat fluxes for a particular area. As has been shown in this section, the time period over which these fluxes are averaged is also important.



#### 4. SURFACE WIND STRESS

Possibly the most important new measurement to be obtained is the surface wind stress vector using the SEASAT scatterometer. Since the rate at which turbulent energy is provided to the ocean by the surface wind is proportional to wind speed cubed (Eq. 8), it is important that this term be known accurately over a large area. The discontinuous coverage by satellites again leads to some difficulty because of the strongly non-linear dependence of the mixed-layer deepening rate on the wind speed. In this section the effects of wind stress magnitude and wind stress direction will be discussed.

Figure 8 shows the effect of an impulsive wind event during a one month period. The solid curve shows the rate of deepening for a constant heat flux with a constant wind speed of  $5 \text{ m sec}^{-1}$ , except that the wind speed is  $20 \text{ m sec}^{-1}$  from day 10 to day 13. During this impulsive event the mixed-layer deepens rapidly to about 80 m and then levels off for the remainder of the month. If the satellite observes surface winds ten times during the month and if nine of the observations are speeds of  $5 \text{ m sec}^{-1}$  and one of  $20 \text{ m sec}^{-1}$ , then deepening is given by the solid curve if each observation is assumed to persist for the following three days. If the average monthly wind speed is computed and inserted into the model the deepening for the month is given by the dashed curve, and it is apparent that considerably less deepening occurs than for the impulsive case. Quite possibly the storm duration or impulsive event would be less than three days, and the actual depth at the end of the period would be between 50 and 85 m. However, without additional information it is not possible to ascertain the true situation, although spatial and temporal correlations over an ocean basin might provide additional information about wind speeds during impulsive events. The third curve in Fig. 8 shows the deepening rate when the average of the wind speed cubed is used in the model simulation. The final depth in this case compares favorably with the impulsive deepening case. Some improvement over these results would be obtained by insertion of SEASAT winds since 20 measurements will be obtained each month due to the 36 hr repeat cycle.

Directional information as well as speed will be provided by the SEASAT scatterometer. Figure 9 shows that the rate of mixed-layer deepening may depend on the direction of the surface wind stress in addition to the magnitude whenever an initial current is present. With an initial geostrophic current,  $u_g$ , in the x-direction, the time-dependent horizontal current velocity due to an imposed wind stress can be determined from the horizontal momentum equations and is given by Niiler (1975) as

$$\begin{aligned}\bar{u} &= \frac{\tau}{\rho f h} \sin f t + u_g \\ \bar{v} &= \frac{\tau}{\rho f h} (\cos f t - 1)\end{aligned}\tag{11}$$

where  $\tau$  is the surface stress and  $f$  is the Coriolis parameter. Figure 9 shows that the deepening rate differs over a one day period depending on whether the stress is in the positive or negative x-direction. When the stress is in the same direction as  $u_g$ , the deepening is more rapid particularly during the first six hours during which the stress is imposed. Hence, satellite observations of wind direction would be useful for determining deepening for inertial time scales during which the term  $(1 - m_s) \frac{\bar{u}^2}{2}$  in Eq. (8) is important.

Since the surface wind speeds will be available on a regular basis during the cooling season, it is essential that the relative importance of forced and free convection be known. Changes in the amount of heat stored in the upper ocean may occur rapidly during the cooling season. With  $m_s = 1$ ,  $m_b = 0$ ,  $R = 0$ , Eq. (8) reduces to

$$\frac{dh}{dt} = \frac{2(m - m_p) u_*^3}{-a g h (T - T_h)} + \frac{m_c F}{(T - T_h)}\tag{12}$$

as the mixed-layer erodes during autumn cooling. Hence, the relative importance of forced and free convection depends on the values of the constants  $m - m_p$  and  $m_c$ . An analysis of observational data could provide the values of these constants. Figure 10 is a schematic

diagram that shows how SEASAT wind stress data can be used to predict the heat storage in the upper ocean in real time when information about the sea surface temperature from the SEASAT SMMR is also provided. If the model is capable of correctly predicting the changes in heat storage, an additional valuable piece of information will be available – the surface heat flux. Knowledge of the surface heat flux would be extremely beneficial for comparison with satellite derived bulk parameterizations of these fluxes. As shown in Fig. 10, it is essential to know whether the deepening is primarily due to forced convection or free convection during the time period. The equations for changes in  $\Delta h$  in Fig. 10 are based on Eq. (8) with  $m_s = 1$ ,  $m_b = 0$ ,  $R = 0$  and assuming  $\frac{\partial T}{\partial z} = 0$  below the mixed-layer.

## 5. ADVECTIVE EFFECTS

The one-dimensional mixed-layer model used in the previous simulations has not included any mechanism to provide horizontal coupling between grid points. On seasonal and annual time scales horizontal advection is important, and a natural extension of the one-dimensional model can be considered. It may be possible to derive ocean surface currents from wave spectra data to be observed by the synthetic aperture radar (SAR) on SEASAT. If so this information would be extremely valuable in assessing the relative importance of horizontal heat transports in various oceanic regions.

Horizontal advection can be included in the model at a specific grid point by assuming the existence of a temperature gradient in the x-direction and a mean mixed-layer velocity  $\bar{u}$ . Then the integrated form of Eq. (1) will include an advective term. Figure 11 shows how horizontal advection, with  $\bar{u} = 15 \text{ cm sec}^{-1}$  and  $\frac{\partial T}{\partial x} = -1^\circ \text{C}/250 \text{ km}$ , affects the rate of mixed-layer deepening. For the case shown, the horizontal advection is assumed to occur over a depth  $D$ , which is less than the mixed-layer depth. Hence, the advective temperature change over the mixed-layer is given by

$$\Delta T_{adv} = - \frac{D}{H} \bar{u} \frac{\partial T}{\partial x} . \quad (12)$$

For both curves the net heat flux is the same over the 30 day period, but when horizontal advection of warmer water is allowed, less deepening occurs. The deepening is reduced when warm advection occurs because the surface layer is warmed which in turn increases the temperature difference,  $T - T_b$ , across the bottom of the mixed-layer. Since the deepening rate is inversely proportional to  $T - T_b$ , the deepening rate is reduced.

The important point to note here is that the horizontal advection alters the dynamics of the deepening mixed-layer. Simply adding the advective temperature change at the end of the 30 day period does not yield the same result as including the advective temperature change at each time step. To fully understand the effects of horizontal advection on these one-dimensional models, it is necessary to consider models with numerous horizontal grid points which can interact with each other through the advective terms in the equations.

## 6. SUMMARY AND CONCLUSIONS

Satellites such as SEASAT-A will provide information, for the first time, that will allow changes in heat storage of the upper ocean to be predicted in real time on seasonal and annual time scales. Since satellites can observe parameters at the ocean surface, it is particularly appropriate to consider a model which predicts changes in the upper ocean and assumes a steady state in the region below. Such a model is unlikely to be suitable for time scales much longer than an annual cycle unless further modifications are included. The sensors aboard the new generation of oceanographic satellites will provide measurements of sea surface temperature, surface heat fluxes, vector winds and surface currents: all of which are important variables in models of the surface mixed-layer.

A mixed-layer model has been studied to determine how physical parameters measured from satellites affect the heat storage in the upper ocean. One major problem associated with the insertion of satellite data into the model arises due to the discontinuous nature of the coverage. The principal conclusions of the present study can be summarized as follows:

1. Annual Cycle. Annual cyclic states can be obtained by making certain assumptions about the dissipation term in the turbulent mechanical energy equation. If  $m_c$  is decreased from 1 to 0, penetrative convection due to surface cooling is reduced, and this causes a reduction in mixed-layer deepening during the cooling season. If in addition,  $m - m_p$  becomes smaller for deeper depths, then annual cyclic states are obtained. Another method of obtaining annual cyclic states is to assume the existence of a constant background dissipation ( $m_b > 0$ ). Further work is necessary to find the values and possible variations of the parameters  $m_c$ ,  $m - m_p$  and  $m_b$ .

2. Diurnal Cycle and Data Averaging. When heat fluxes are averaged over different time periods during a diurnal cycle, different mixed-layer depths and sea surface temperatures are obtained. This is due to the non-linear form of the model as well as the penetrative convection parameter. This result is particularly important with respect to satellite measurements which are not continuous in time and hence must be averaged over some interval. It is important to determine over what averaging interval the model predictions will be accurate.

3. Vector Wind Stress. Both the magnitude and the direction of the surface wind stress will be available from the SEASAT scatterometer, and both are important in determining mixed-layer deepening. Since deepening is proportional to wind speed cubed, it is particularly important to know the duration of impulsive events. The direction of the surface wind stress is shown to be important in determining the deepening rate on short time scales whenever an initial current exists.

4. Forced and Free Convection. It is necessary to determine the relative contributions of forced and free convection to mixed-layer deepening during the cooling season. Further analysis of observational data is necessary to get this information. An algorithm is given to predict the upper ocean heat storage in real time given the wind stress measurements from the SEASAT scatterometer and the sea surface temperature from the SEASAT SMMR. An additional output will be a value for the heat flux between successive satellite passes. This

can be compared with satellite derived fluxes using the standard bulk aerodynamic formulation.

**5. Horizontal Advection.** In regions of strong currents, changes in heat storage will depend on horizontal advection as well as changes in mixed-layer depth. The two effects are not simply additive since the advection affects the dynamics of the deepening mixed-layer. It may be possible to extract useful information about ocean surface currents from the SEASAT synthetic aperture radar.

If parameters such as surface heat fluxes, vector wind stress and horizontal currents can be measured accurately from satellites, these measurements can be used as inputs for models which predict the seasonal or annual evolution of the heat storage in the upper ocean. Accurate real time prediction of this heat storage would be invaluable to climate modelers who wish to predict climatic variations on seasonal or annual time scales.

## **ACKNOWLEDGMENTS**

I would like to thank Dr. James L. Mueller for many helpful discussions and comments during the preparation of this report. The bulk of this research was completed while the author was a participant in the NASA/ASEE Summer Faculty Fellowship Program sponsored by the University of Maryland and Howard University.

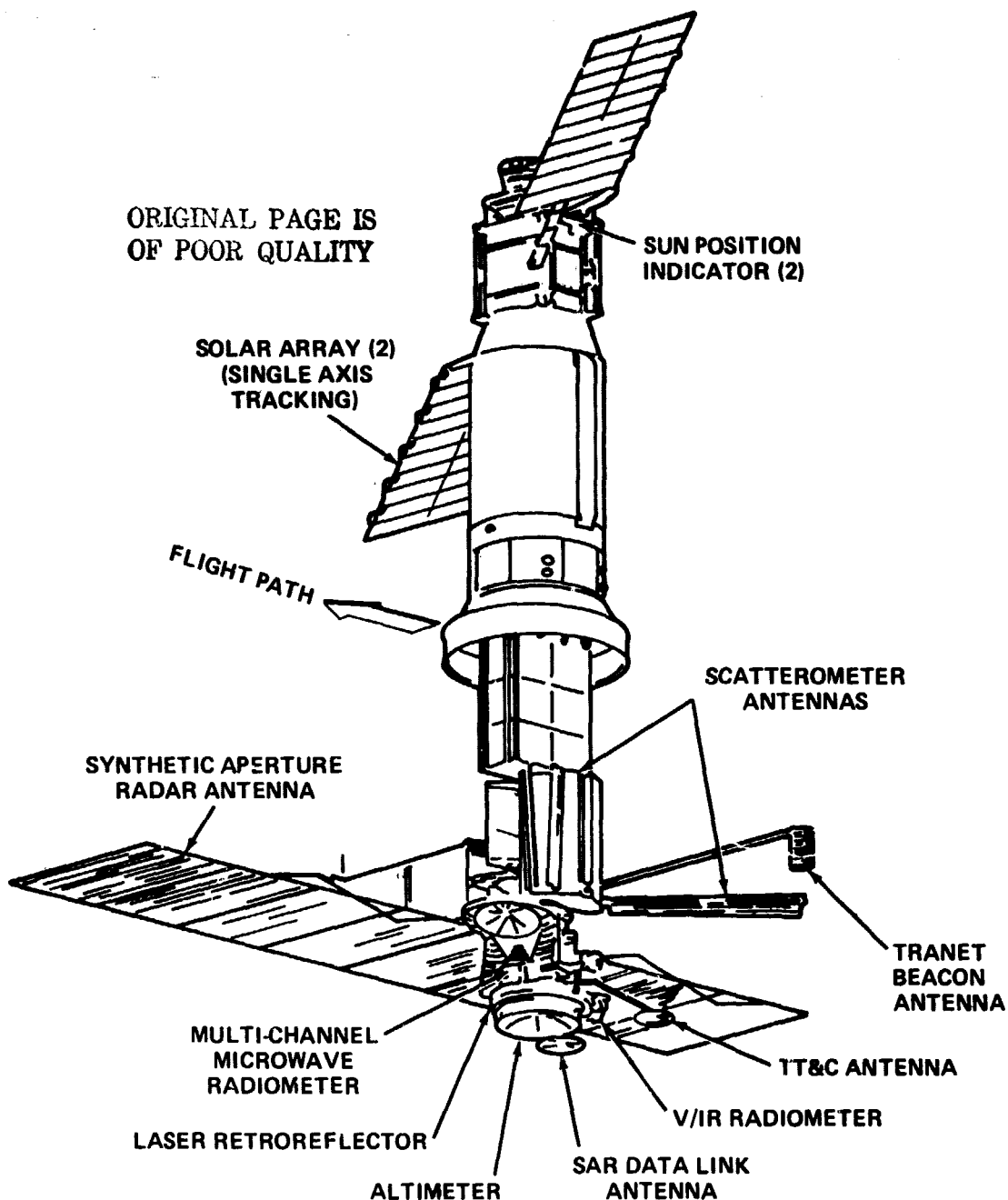


Figure 1. Flight Configuration of SEASAT-A with Location of Various Sensors

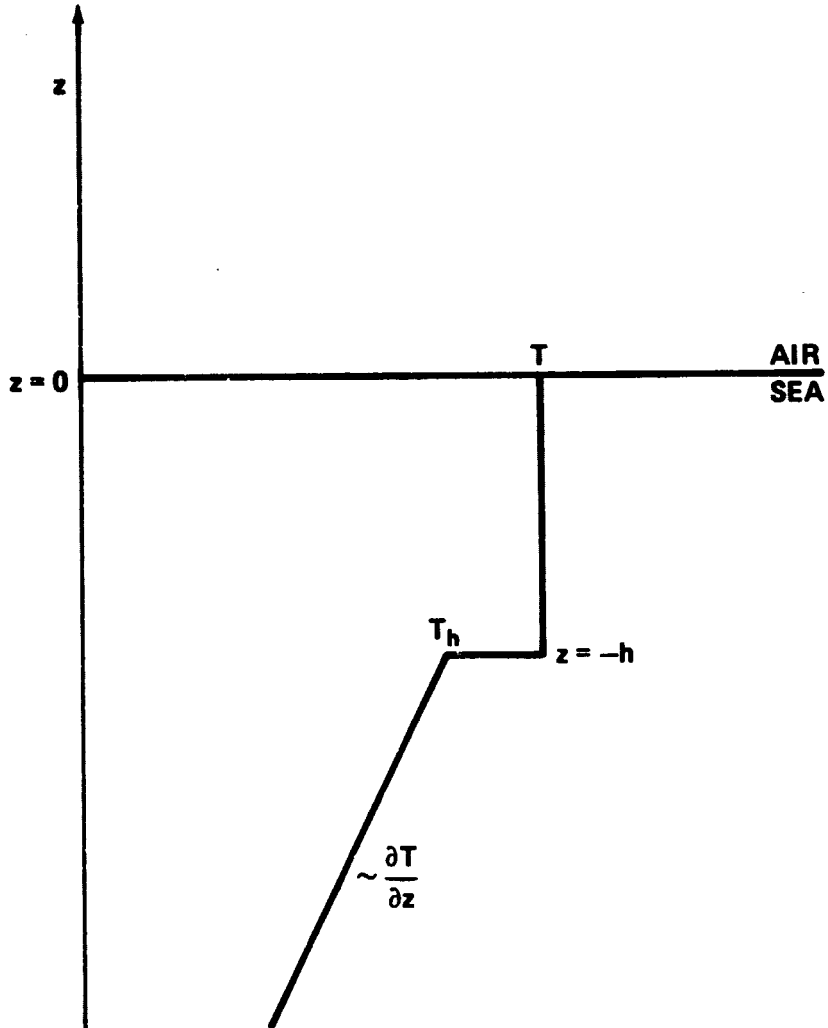


Figure 2. Schematic Representation of the Temperature Profile Assumed in the Mixed-Layer Model. Relevant Parameters Are the Sea Surface Temperature ( $T$ ), the Mixed-Layer Depth ( $h$ ), the Temperature Immediately Below the Mixed-Layer ( $T_h$ ), and the Temperature Gradient  $\left(\frac{\partial T}{\partial z}\right)$  in the Lower Region.



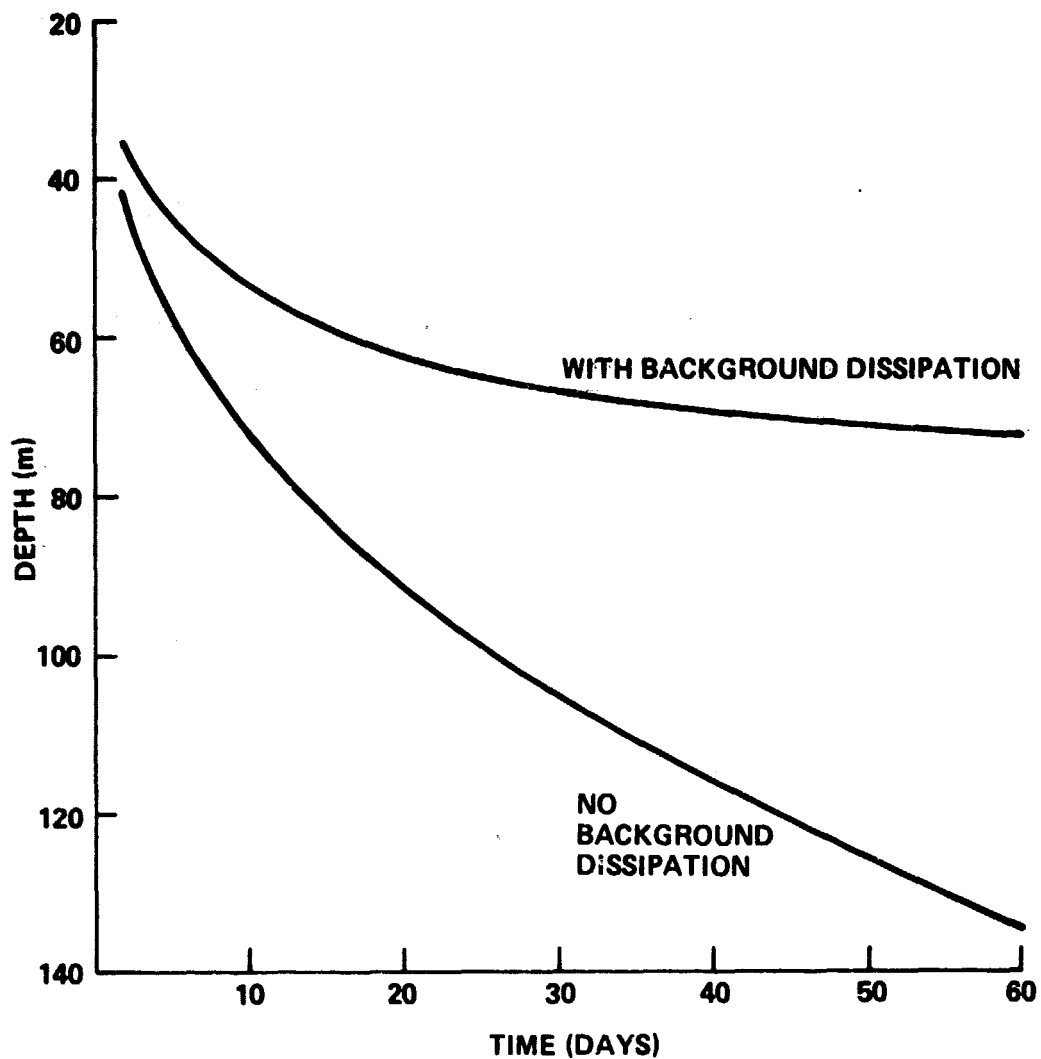


Figure 3. Comparison of Mixed-Layer Deepening With and Without Background Dissipation. There is No Net Heating and the Wind Speed is Constant at  $10 \text{ m sec}^{-1}$ .

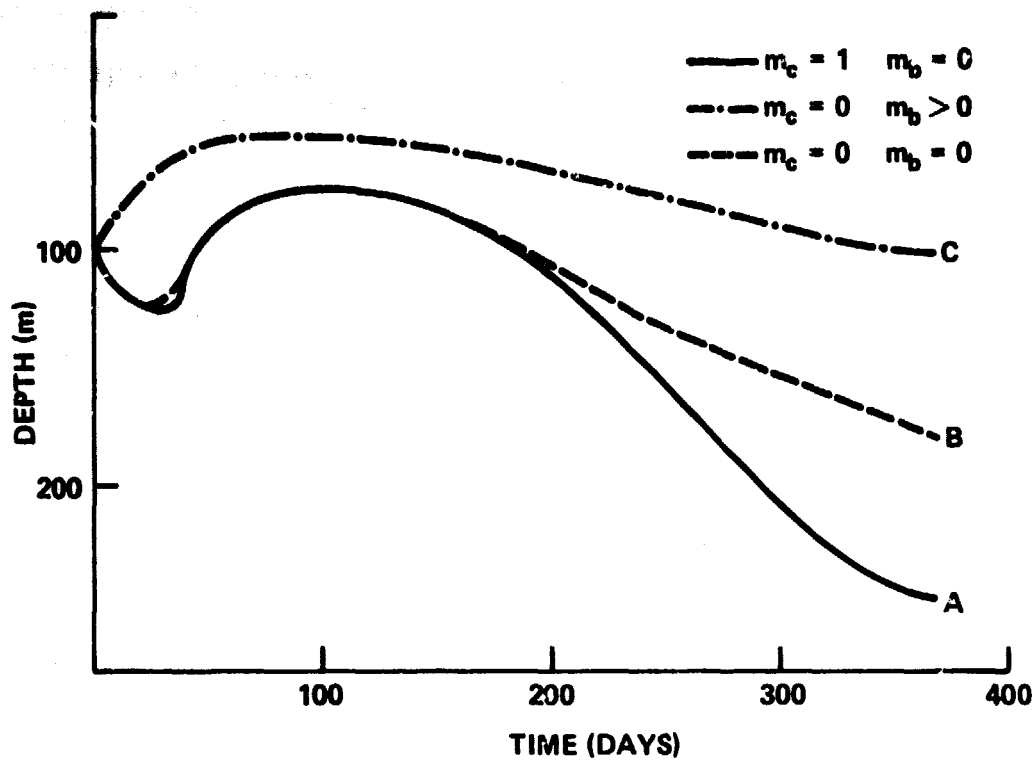


Figure 4. Variations in Annual Cyclic States Due to Changes in the Background Dissipation and Penetrative Convection Terms. The Heat Flux is Sinusoidal with a One-Year Period and an Amplitude of  $400 \text{ cal cm}^{-2}\text{day}^{-1}$ . The Wind Speed is  $10 \text{ m sec}^{-1}$ .

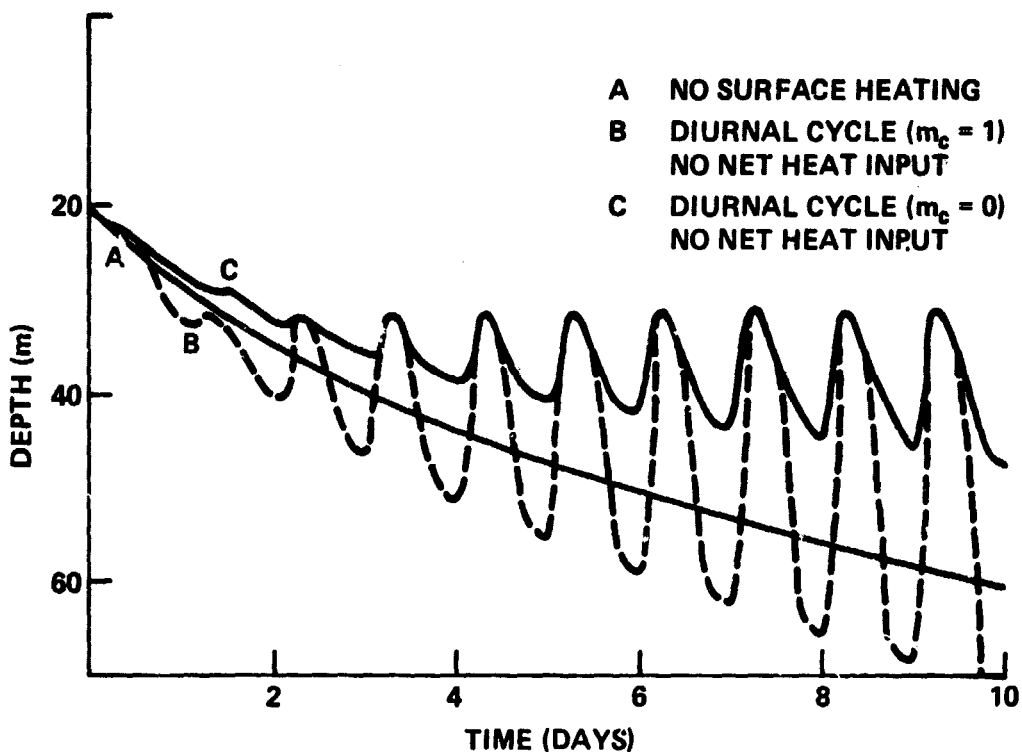


Figure 5. Variations in Deepening Rates Due to Changes in the Averaging Interval for the Surface Heat Fluxes. The Net Heating is Zero and the Wind Speed is  $8 \text{ m sec}^{-1}$ . For Curve A, the Heat Flux is Zero Throughout the Period While the Heat Flux Varies Sinusoidally with an Amplitude of  $960 \text{ cal cm}^{-2} \text{ day}^{-1}$  and an Averaging Interval of 1.2 Hours for the Other Two Curves.

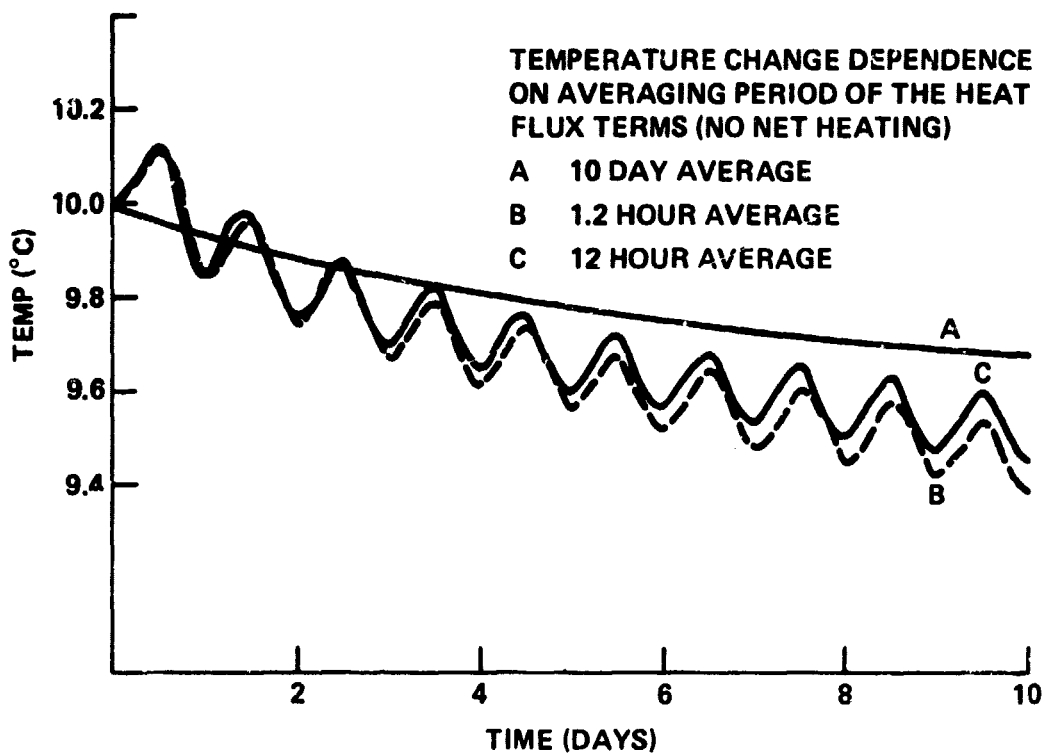


Figure 6. Variations of Sea Surface Temperature Due to Using Different Averaging Periods for the Surface Heat Fluxes ( $m_b = 0$ ,  $m_c = 1$ ).

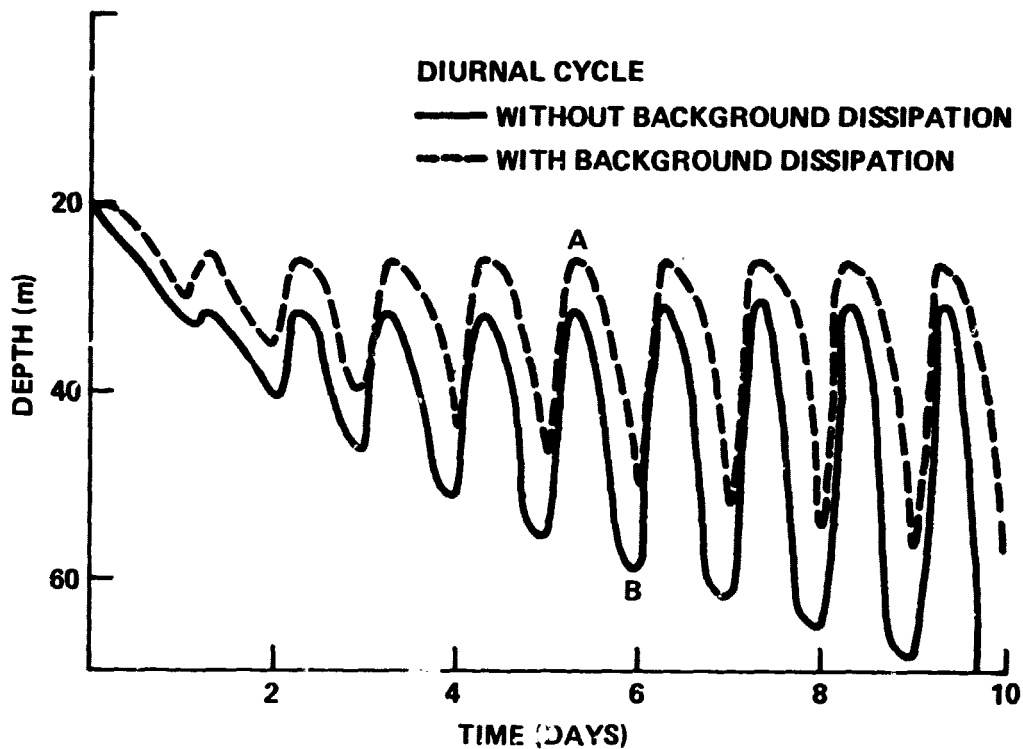


Figure 7. Variations in Mixed-Layer Deepening Over Ten Diurnal Cycles With and Without Background Dissipation. Curve B is the Same as Curve B in Figure 5.

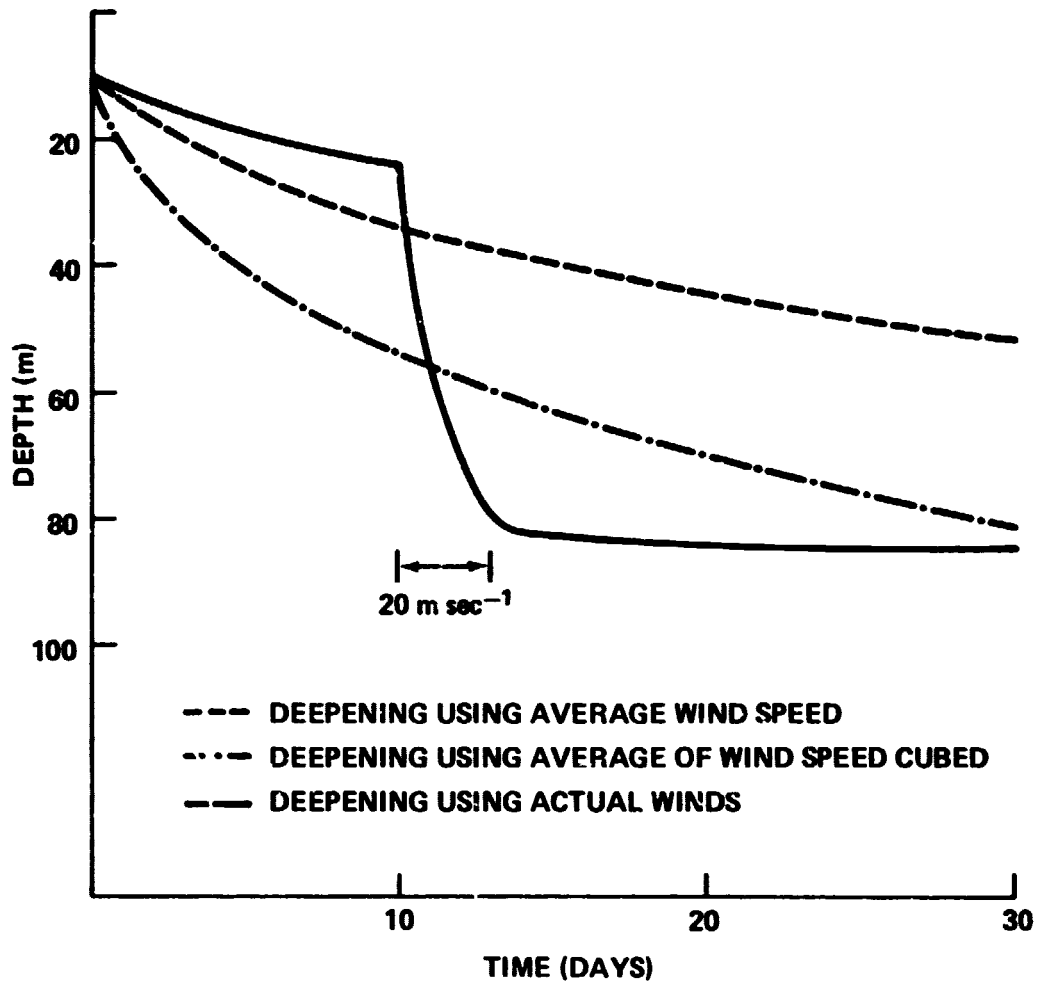


Figure 8. Solid Curve Shows Mixed-Layer Deepening Due to an Impulsive Wind Stress with  $u = 5 \text{ m sec}^{-1}$  Except During the Impulsive Event. The Other Two Curves Show the Different Deepening Rates When Different Averaging Methods Are Used.

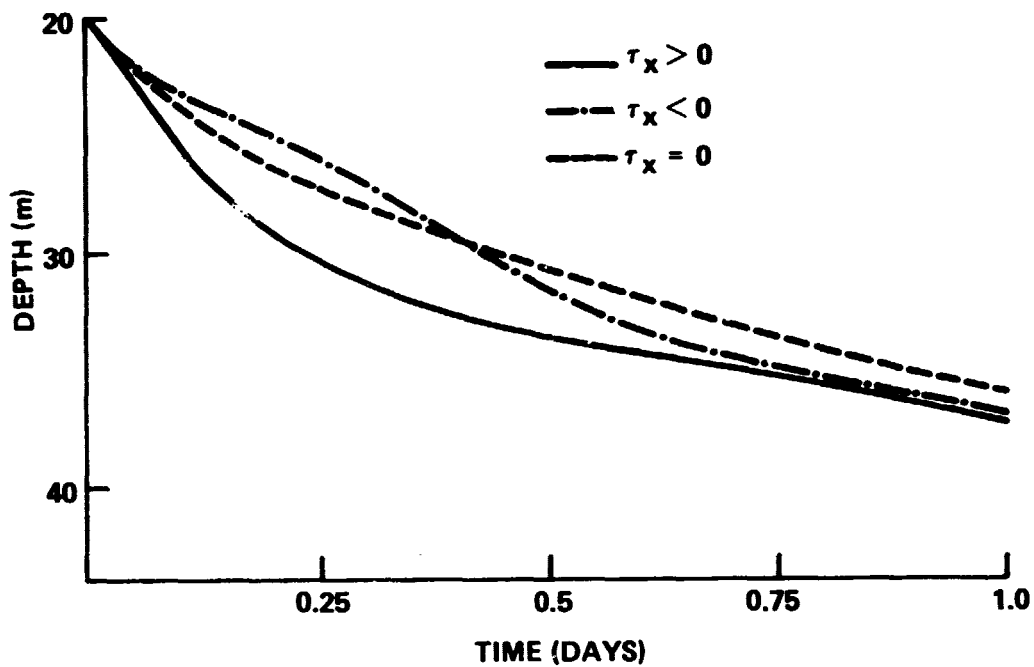


Figure 9. Effect of Wind Direction on the Mixed-Layer Deepening Rate When a  $10 \text{ cm sec}^{-1}$  Current in the Positive x-Direction is Initially Present.

ORIGINAL PAGE IS  
OF POOR QUALITY

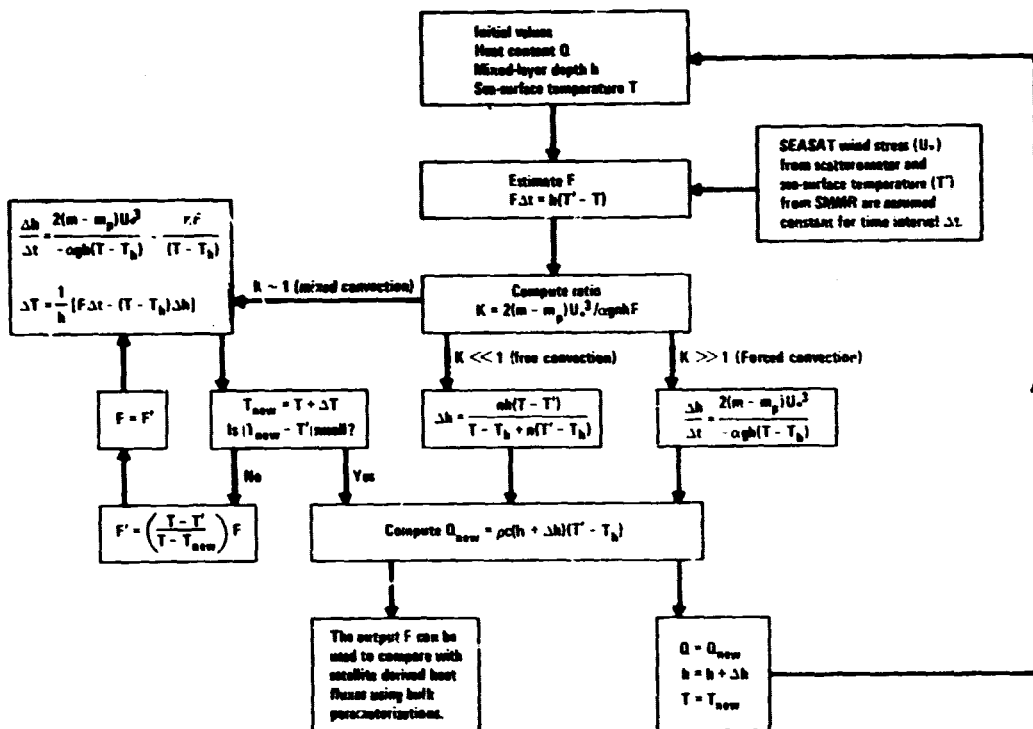


Figure 10. Schematic Diagram of an Algorithm for Predicting Real Time Changes of the Heat Storage of the Upper Ocean Using SEASAT Wind Speed and Sea Surface Temperature Data. An Additional Output is a Measure of the Heat Flux Between Successive Satellite Passes. This Case is for a Cooling Regime with  $\frac{\partial T}{\partial z} = 0$  Below the Mixed-Layer and Assuming a Time Interval of One Unit.



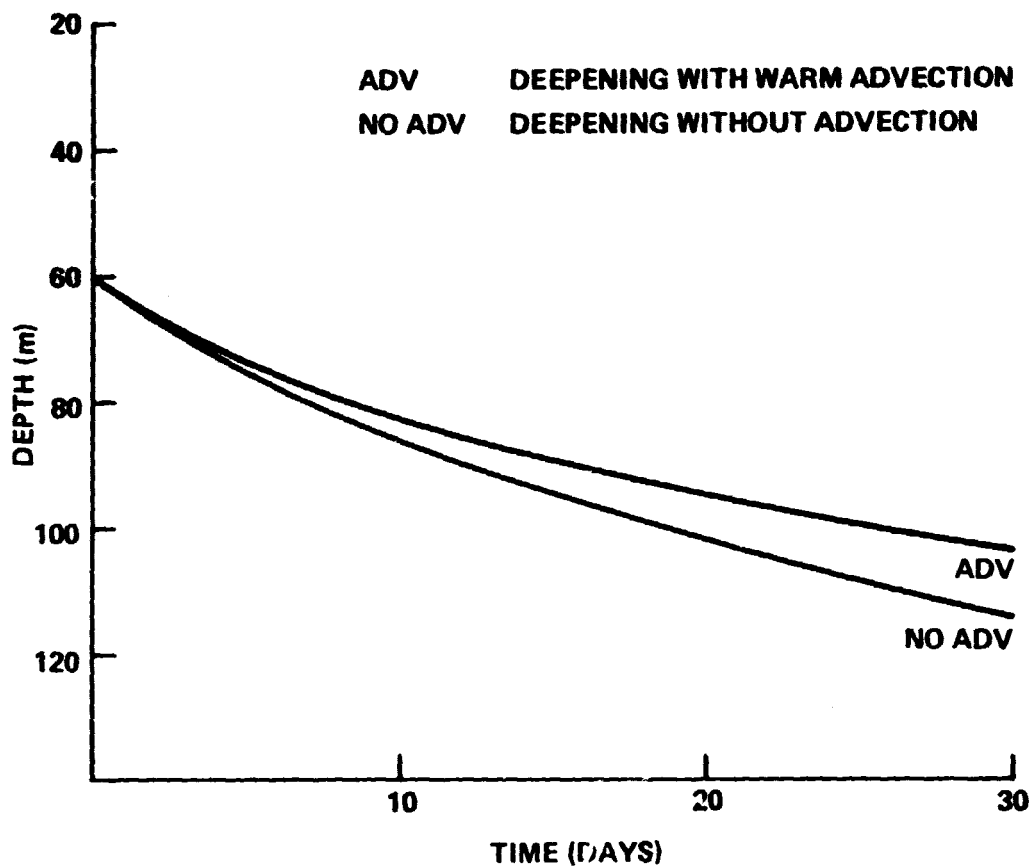


Figure 11. Variation in Mixed-Layer Depth Due to the Advection of Warmer Water Through the Region.

## REFERENCES

- Alexander, R. C., and J. W. Kim, 1976: Diagnostic model study of mixed-layer depth in the summer North Pacific. *J. Phys. Oceanog.*, 6, 293-298.
- Denman, K. L. 1973: A time-dependent model of the upper ocean. *J. Phys. Oceanog.*, 3, 173-184.
- Gill, A. E., and J. S. Turner, 1976: A comparison of seasonal thermocline models with observation. *Deep-Sea Res.*, 23, 391-401.
- Jerlov, N. G., 1968: *Optical Oceanography*, Elsevier, Amsterdam.
- Kim, J., 1976: A generalized bulk model of the oceanic mixed-layer. *J. Phys. Oceanog.*, 6, 686-695.
- Kraus, E. B., and J. S. Turner, 1967: A one-dimensional model of the seasonal thermocline, Part II. *Tellus*, 19, 98-105.
- Miller, J. R., 1976: The salinity effect in a mixed-layer ocean model. *J. Phys. Oceanog.*, 6, 29-35.
- Munk, W. H., and E. L. Anderson, 1948: Notes on a theory of the thermocline. *J. Marine Res.*, 7, 276-295.
- Niiler, P. P. 1975: Deepening of the wind-mixed layer. *J. Marine Res.*, 33, 405-422.
- Niiler, P. P. and E. B. Kraus, 1977: One-dimensional models of the upper ocean. In *Modeling and Prediction of the Upper Layers of the Ocean* (edited by E. B. Kraus). Pergamon Press, 325 pps.
- Phillips, O. M. 1966: *The Dynamics of the Upper Ocean*. Cambridge University Press, 264 pp.

Pollard, R. T., P. B. Rhines and R. O. R. Y. Thompson, 1973: The deepening of the wind-mixed layer. *Geophys. Fluid Dyn.*, 3, 381-404.

Thompson, R. O. R. Y., 1976: Climatological numerical models of the surface mixed-layer of the ocean. *J. Phys. Oceanog.*, 6, 496-503.

Wyatt, L. R., 1976: Mixing and stratifying processes in the oceanic surface layer and seasonal thermocline. Ph.D. Thesis, Univ. of Southampton.

## BIBLIOGRAPHIC DATA SHEET

1. Report No. TM 79601	2. Government Accession No.	3. Recipient's Catalog No.	
4. Title and Subtitle  MONITORING CHANGES IN UPPER OCEAN HEAT STORAGE FROM SATELLITES		5. Report Date July 1978	
		6. Performing Organization Code	
7. Author(s) James R. Miller, Department of Meteorology and Physical Oceanography, Cook College, Rutgers University, New Brunswick, New Jersey 08903		8. Performing Organization Report No.	
9. Performing Organization Name and Address Hydrospheric Sciences Branch NASA Goddard Space Flight Center Greenbelt, MD 20771		10. Work Unit No.	
		11. Contract or Grant No.	
		13. Type of Report and Period Covered  Technical Memorandum	
12. Sponsoring Agency Name and Address		14. Sponsoring Agency Code	
15. Supplementary Notes			
16. Abstract The development of new oceanographic satellites such as SEASAT-A will provide measurements applicable to studies of heat storage changes in the upper ocean on seasonal and annual time scales. A one-dimensional model of the upper ocean mixed-layer has been developed to determine how the parameters which can be measured from satellites affect the development of the layer. The results show that the form of the dissipation term is important in achieving cyclic annual states, that the layer deepening rate depends on the averaging period for the surface heat flux and wind stress, that wind direction, as well as magnitude, can affect the deepening rate and that horizontal advective effects cannot simply be superimposed on the model results. An algorithm is given which uses satellite derived wind stress and sea surface temperature data to predict real time changes in upper ocean heat storage during the cooling seasons.			
17. Key Words (Selected by Author(s))  Ocean Heat Storage, SEASAT, Scatterometer, Microwave Remote Sensing, Upper Ocean Models		18. Distribution Statement  Unlimited	
19. Security Classif. (of this report)  UNCLASSIFIED	20. Security Classif. (of this page)  UNCLASSIFIED	21. No. of Pages	22. Price *